Earth and Planetary Science Letters 309 (2011) 21–32

Contents lists available at ScienceDirect

Earth and Planetary Science Letters

journal homepage: www.elsevier.com/locate/epsl

In-situ cosmogenic ^{10}Be production rate at Lago Argentino, Patagonia: Implications for late-glacial climate chronology

Michael R. Kaplan [a,*], Jorge A. Strelin [b], Joerg M. Schaefer [a,c], George H. Denton [d], Robert C. Finkel [e,f], Roseanne Schwartz [a], Aaron E. Putnam [d], Marcus J. Vandergoes [d,g], Brent M. Goehring [a], Scott G. Travis [h]

[a] Lamont-Doherty Earth Observatory, Geochemistry, Palisades, NY 10964, USA
[b] CICTERRA, Universidad Nacional de Córdoba, Instituto Antártico Argentino, Argentina
[c] Department of Earth and Environmental Sciences, Columbia University, New York, NY 10027, USA
[d] Dept. of Earth Sciences and Climate Change Institute, University of Maine, Orono, ME 04469, USA
[e] Dept. of Earth and Planetary Sciences, University of California, Berkeley, CA 95064, USA
[f] CEREGE, 13545 Aix-en-Provence, Cedex 4, France
[g] GNS Science, P.O. Box 30-368, Lower Hutt 5040, New Zealand
[h] GCI, Soldiers Grove, WI 54655, USA

ARTICLE INFO

Article history:
Received 11 December 2010
Received in revised form 14 June 2011
Accepted 20 June 2011
Available online 23 July 2011

Editor: Y. Ricard

Keywords:
^{10}Be
production rate
cosmogenic nuclide
exposure dating
South America
late glacial

ABSTRACT

When calculated with the commonly accepted average Northern Hemisphere production rate, ^{10}Be dates of surface boulders on moraines in the Lago Argentino area of Patagonia are younger than minimum-limiting ^{14}C ages for the same landforms. This disagreement could result from the lack of a regional ^{10}Be production-rate calibration site. To assess this possibility, we here present high-precision measurements of ^{10}Be in samples collected from surface boulders on the Herminita and Puerto Bandera moraine complexes deposited alongside Lago Argentino on the eastern flank of the Andes at 50°S in Patagonia. Together with maximum- and minimum-limiting ^{14}C ages for the two moraine systems, these measurements confine the local ^{10}Be production rate to between 3.60 and 3.82 atoms/g/yr (midpoint = 3.71 ± 0.11 atoms/g/yr) when using a time-dependent scaling method that incorporates a high-resolution geomagnetic model. This range includes upper and lower error bounds of acceptable production rates derived from both the Herminita and the Puerto Bandera sites. The upper limit of this range is more than 12% below the average Northern Hemisphere production rate, as calculated using the same scaling method, given in Balco et al. [Quat. Geochron 3 (2008) 174–195]. Other scaling models yield production rates with similarly large offsets from the Balco et al. (2008) rate. On the other hand, the range of acceptable production rate values determined from Patagonia overlaps at 1σ with, and encompasses, the production rate recently derived in Macaulay valley in the Southern Alps of New Zealand [A. Putnam et al., Quat. Geochron. 5 (2010a) 392–409]. Within uncertainties (i.e., overlap at 1 sigma) this Patagonian production rate range also agrees with a recently determined production rate from low-elevation sites in northeastern North America and northern Norway. When the Macaulay production rate is used to calculate Patagonian exposure dates, ^{14}C and ^{10}Be chronologies are mutually compatible for late-glacial moraine systems. Both chronologies then indicate that outlet glaciers of the Southern Patagonian Icefield achieved a late-glacial maximum in the western reaches of Lago Argentino at 13,000 cal. yr BP at the end of the Antarctic Cold Reversal (14,500–12,900 cal. yr BP). Outlet glaciers subsequently receded to near present-day ice margins during the Younger Dryas stadial (12,900–11,700 cal. yr BP). This general retreat was interrupted about 12,200 cal. yr BP when Upsala Glacier constructed an interlobate complex of moraine ridges on Herminita Peninsula. Mountain glaciers in Patagonia and New Zealand, on both sides of the South Pacific Ocean, exhibited a coherent pattern of late-glacial ice-margin fluctuations.

1. Introduction

Climate changes in the Southern Hemisphere during the last transition from glacial to interglacial conditions remain poorly understood. Ice cores at high southern latitudes register the Antarctic Cold Reversal (ACR, 14,500 to 12,900 cal. yr BP) as a plateau or a reversal in temperature and in atmospheric CO_2 concentration (Blunier et al., 1997; EPICA, 2004; Jouzel et al., 2001; Stenni et al., 2011). Antarctic temperature and atmospheric CO_2 then increased (Blunier et al., 1997; EPICA, 2004) during the Younger Dryas stadial (YD, 12,900 to 11,700 cal. yr BP) of the North Atlantic region. In the Southern Alps of New Zealand in middle latitudes, glacier expansion occurred during the ACR and recession

* Corresponding author.
E-mail addresses: mkaplan@ldeo.columbia.edu, kaplanm2001@yahoo.com (M.R. Kaplan).

0012-821X/$ – see front matter © 2011 Elsevier B.V. All rights reserved.
doi:10.1016/j.epsl.2011.06.018

during the YD (Alloway et al., 2007; Kaplan et al., 2010; Putnam et al., 2010b). An outstanding question is whether the timing of glacier advance and retreat observed in New Zealand is evident in enough other areas of the middle latitudes to imply a coherent pattern of late-glacial climate change over the southern half of the Southern Hemisphere.

Whether glaciers in South America advanced or retreated during the ACR and the YD is a matter of debate (Ackert et al., 2008; Kaplan et al., 2008; Mercer, 1976; Moreno et al., 2009; Strelin and Denton, 2005; Sugden et al., 2005). For example, Ackert et al. (2008) produced a large and internally consistent set of ^{10}Be and ^{36}Cl exposure ages for a moraine ridge of the classic late-glacial Puerto Bandera landform sequence alongside Lago Argentino (50°S). The data set obtained by Ackert et al. (2008) was taken to mean that at least one of the Puerto Bandera lobes deposited moraines in earliest Holocene/latest YD time, in contrast to the older age for Puerto Bandera moraines inferred from ^{14}C dating (Mercer, 1976; Strelin et al., in press; Strelin and Denton, 2005; Strelin and Malagnino, 2000). This chronological discrepancy may reflect the lack of a local production rate for determining accurate ^{10}Be surface-exposure dates. Therefore, we investigate here the ^{10}Be production rate in Patagonia and discuss the implications for late-glacial climate changes.

Two primary methods are used here to date glacial deposits in Patagonia, ^{14}C and cosmogenic exposure dating. Prior to the late CE1990s, only ^{14}C ages on organic matter afforded mainly minimum-limiting values for glacial tills and/or landforms. However, over the last 15 years, cosmogenic nuclide measurements of samples from surface boulders have been used to determine the exposure age of moraine systems (e.g., Ackert et al., 2008; Jackofsky et al., 1999; Kaplan et al., 2008; McCulloch et al., 2005; Moreno et al., 2009). Such cosmogenic ages should pinpoint when a boulder was deposited on a moraine ridge. But an accurate cosmogenic nuclide age for the boulder under question requires knowledge of the in-situ accumulation rate of ^{10}Be atoms near the upper rock surface.

At present, the production rate of ^{10}Be at different latitudes and elevations is debated (e.g., Balco et al., 2008; 2009; Fenton et al., in press; Putnam et al., 2010a). In the middle-to-high latitudes of the Southern Hemisphere, there is only a single ^{10}Be production-rate calibration site, situated in Macaulay valley of the Southern Alps of New Zealand (Putnam et al., 2010a). The Macaulay ^{10}Be production rate is 12–14% lower than the widely used Northern Hemisphere "average" value (Balco et al., 2008), which is based on all geological ^{10}Be calibration sites employed before CE2008. However, recently published ^{10}Be production-rate values from the Northern Hemisphere, one from northeastern North America (Balco et al., 2009) and another from northern Norway (Fenton et al., in press), are consistent with the Macaulay rate, within stated uncertainties. In southern South America, a local ^{10}Be calibration site is not yet available. Therefore, whether the ^{10}Be production rate commonly used in the Northern Hemisphere (Balco et al., 2008) or that obtained in Macaulay valley of New Zealand, or neither, should be employed in Patagonia remains unresolved.

Here, we test what production rate should be used to calculate ^{10}Be surface-exposure ages in Patagonia. To accomplish this test, we measure ^{10}Be concentrations in boulders on moraines with independent limiting ^{14}C ages in the Lago Argentino area of Patagonia. We document at two different localities that ^{14}C- and ^{10}Be-based chronologies for moraine formation are mutually compatible only if the Macaulay production rate is employed in the exposure-age calculations. After demonstrating the appropriate production rate to be used in Patagonia, we show that both the ^{14}C and the ^{10}Be techniques afford consistent ages for glacier fluctuations, together indicating expansion during ACR and contraction during YD times.

2. Background

2.1. Setting and climate

The southern Andes support the 16,800 km^2 Southern Patagonian Icefield (SPI). Outlet glaciers that drain the SPI include the Perito Moreno, Upsala, Grande, and Dickson Glaciers (Fig. 1A). These glaciers terminate near the western reaches of Lago Argentino (50°S, 72°W), the second largest lake in Patagonia. The eastern end of the main body

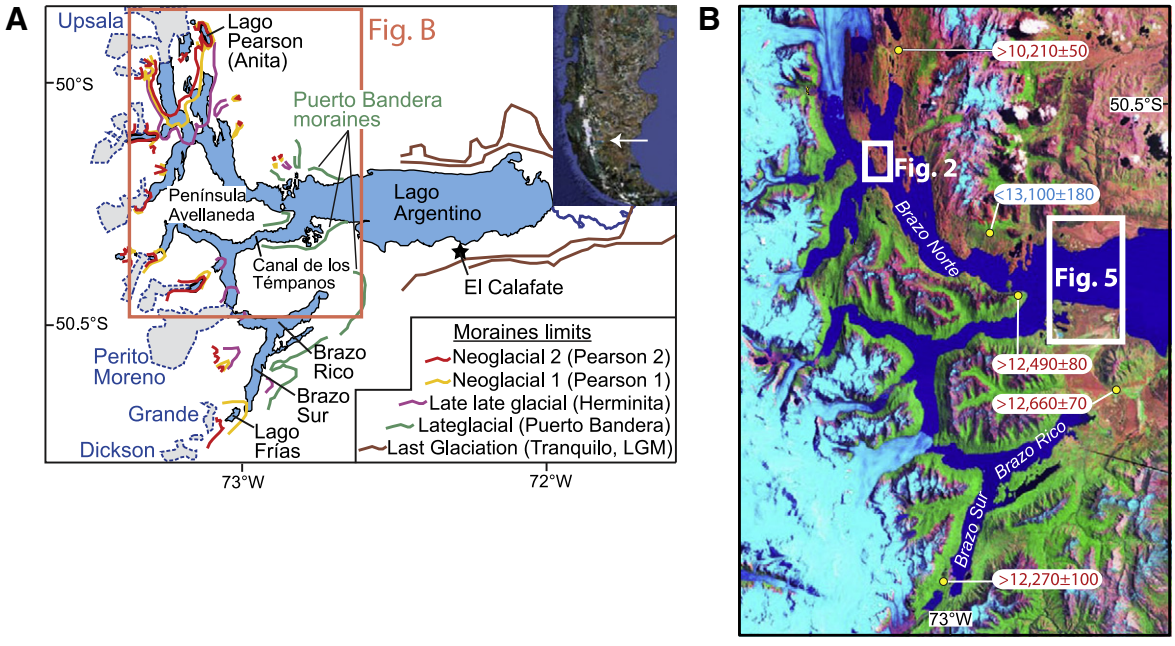

Fig. 1. A) Map of the Lago Argentino area with places mentioned in the text and the major moraine systems drawn schematically (Mercer, 1968, 1976; Strelin and Malagnino, 2000; and references therein); B) A satellite image that shows the Lago Argentino area, including the setting of the Herminita Peninsula (Fig. 2) and outlet glaciers of the SPI. Minimum-limiting calendar-year converted ^{14}C ages are shown in red at Península Avellaneda, Brazo Rico spillways, Lago Pearson (Anita) and Lago Frías (see Table 1). Maximum-limiting calendar-year converted ^{14}C age for the Puerto Bandera moraines is shown in blue. ^{14}C dates are from Strelin and Denton (2005), Strelin et al. (2008), and Strelin et al. (in press). Ages reported as cal. yr before present (BP). For production rate calculations (Table 3), 57 or 58 years are added to these calendar-year converted ^{14}C ages, so they are relative to CE2007 and CE2008 (the year in which samples for ^{10}Be analyses were collected).

of Lago Argentino is in a semi-arid steppe environment, which extends through the Santa Cruz River Valley to the Atlantic Ocean. Near the western branches of the lake, the foothills of the Patagonian Andes (Fig. 1) are covered by *Nothofagus* deciduous forest.

The persistent westerlies that cross the cordilleran mountain chain represent the most dominant feature of the present-day climate near Lago Argentino. The position of the westerlies is controlled by the subtropical anticyclone in the southeast Pacific and the circum-Antarctic low-pressure belt (Menéndez et al., 1999; Pittock, 1980). The Andes produce a pronounced orographic climate effect (Clapperton, 1993). As a result, annual precipitation peaks at about 10,000 mm on the mountain divide, but diminishes rapidly eastward to about 200 mm at El Calafate alongside the central sector of Lago Argentino (Casassa and Rivera, 1999; Servicio Meteorológico Nacional).

The study area is located near the Cordillera–Precordillera boundary. West of this transition, the branches of Lago Argentino incise the Patagonian Andes region, exposing Paleozoic metamorphic rocks, Upper Jurassic silicic–volcanic and marine-to-continental sedimentary rocks that formed during a generalized rifting phase, as well as volcaniclastic turbidites and ophiolite successions of the Lower Cretaceous Rocas Verdes Marginal Basin. These rocks are all intruded by Cretaceous to Cenozoic plutonic (largely granitic) bodies (Hervé et al., 2000). To the east of the Cordillera–Precordillera transition, the main water body of Lago Argentino is located in the Precordillera domain, characterized by lower Cretaceous to Tertiary marine-to-continental sedimentary rocks of the Austral (Magallanes) Foreland Basin. No carbonate rocks are described around Lago Argentino that would serve to complicate ^{14}C chronologies.

2.2. Glacial geology

During the last glaciation, outlet glaciers of the Southern Patagonian Icefield expanded, coalesced, and flowed eastward through the basin of present-day Lago Argentino and into the Santa Cruz valley, where El Tranquilo moraines mark the ice limit at the end of the local last glacial maximum (LGM) (Fig. 1A) (Mercer, 1976; Strelin and Denton, 2005; Strelin and Malagnino, 2000). Recession from the El Tranquilo ice limits during the last termination was interrupted in late-glacial time by renewed expansion into the western reaches of Lago Argentino that culminated at the Puerto Bandera moraines (Strelin and Malagnino, 2000; Strelin and Denton, 2005; Ackert et al., 2008 (supplement, Fig. S1)). Following emplacement of the Puerto Bandera moraines, Upsala Glacier receded northward through the Brazo Norte branch of Lago Argentino (Figs. 1 and 2; Strelin et al., in press) during the first half of Younger Dryas time. An interruption in this general recession is registered by the Herminita moraines (Malagnino and Strelin, 1992), which were deposited by Upsala Glacier on the southern tip of Herminita Peninsula, well upvalley from the Puerto Bandera ice-marginal positions. Aniya and Sato (1995) obtained a minimum-limiting ^{14}C age of 2300 ^{14}C yr BP for formation of the Herminita moraines, which Strelin et al. (in press) document are actually older than 10,350 ^{14}C yr BP (Table 1).

Malagnino and Strelin (1992) first described the Herminita moraine complex. The moraine ridges within this complex are interlobate in origin, formed by the confluence of two glacier lobes, one in Brazo Upsala and the other in Brazo Cristina. In plan view, the overall moraine complex has a V-shape, with the point of the V projecting to the northwest (Fig. 2). We mapped as many as five semi-continuous ridges that compose the Herminita moraines (e.g., Figs. 2B and S2). The discontinuous moraine ridges may have been deposited after minor glacier advances or stillstands. Herminita moraine ridges feature numerous large surface erratic boulders, some exceeding 300 m^3 in volume (Malagnino and Strelin, 1992) (Fig. S2). These boulders are of local provenance and consist of lower Cretaceous epyclastic sedimentary rocks (mudstones and sandstones), upper Jurassic volcanites (andesites to rhyodacites), and pre-Jurassic metamorphic rocks (schists). Only the sandstones and rhyodacite lithologies were sampled for ^{10}Be dating.

After formation of the Herminita moraines, the Upsala Glacier receded close to its present-day margin, as summarized below (Section 2.4) (Strelin et al., in press; Strelin and Denton, 2005). Upsala Glacier then advanced in middle-to-late Holocene time to the Pearson 1 and 2 moraine positions (Figs. 1 and 2; Mercer, 1968; Malagnino and Strelin, 1992; Aniya and Sato, 1995; Strelin et al., 2008).

2.3. Glacial isostacy and neotectonics

It is important to determine whether uplift of the land surface has occurred at production-rate calibration sites during the period of exposure to cosmic rays. Because lower atmospheric pressure accompanies surface uplift into higher elevations, this effect exposes the land surface to increasing cosmic-ray fluxes and therefore to greater in-situ ^{10}Be production than would have been the case if surface uplift had not occurred. In this regard, there is no evidence of pronounced glacial isostatic recovery or of significant tectonic uplift of landforms where we collected samples for exposure dating. For example, paleo-shorelines formed since deposition of the Puerto Bandera moraines do not show warping that might reflect significant isostatic recovery with markedly increased uplift rates towards the mountains (Malagnino and Strelin, 1992; Strelin and Malagnino, 1992; unpublished observations). Most of the integrated exposure history of the samples occurred in the Holocene, after disappearance of the large LGM ice lobes (Mercer, 1976; Strelin and Malagnino, 2000). In addition, much of the ice mass lost during recession was replaced by the mass of water in the relatively deep branches (Naruse and Skvarca 2000) and main body of Lago Argentino. Finally, lateral or vertical offsets of former shorelines (or other features such as stream terraces) that would reflect fault movement since formation of the Herminita or Puerto Bandera moraines are not observed at or near the sample sites.

2.4. ^{14}C age constraints for the Herminita moraine system

All pertinent ^{14}C dates are described in Strelin et al. (in press). Here we discuss ^{14}C data directly relevant for constraining the age of the Herminita moraines (Table 1; Figs. 1 and 2). All ^{14}C ages are calibrated to calendar years BP (i.e., before CE1950) based on the IntCal09 curve and the OxCal 4.0.5 program (Reimer et al., 2009), unless otherwise noted.

Core AR0613 was taken through a bog situated a short distance inboard of the northern (inner) mapped limit of the Herminita moraines (Table 1, Figs. 2 and S2E). The lowest dated organic sample in core AR0613, from 5.75 to 5.76 m below the surface, afforded an age of 10,350 ± 45 ^{14}C yr BP (i.e., years before CE1950), which calibrates to a calendar-year age of 12,220 ± 110 cal. yr BP (mean ± 1σ) (Table 1). In the same AR0613 core, above the lowest sample dated to 10,350 ^{14}C yr BP, a second sample from 5.71 to 5.72 m below the surface gave an age of 9950 ± 55 ^{14}C yr BP (11,410 ± 120 cal. yr BP) (Table 1). In addition, a sample of organic material was dated from close to the basal section of nearby cores AR0714, AR0705 and AR0704, one of which (AR0714) is slightly farther inboard of the Herminita moraines than core AR0613 (Fig. 2A). As the 10,350 ^{14}C yr BP date was assayed from a sample collected just above basal sand (Fig. 2A), we conclude that it affords a minimum-limiting value for abandonment of the Herminita moraines by Upsala Glacier.

Another minimum-limiting ^{14}C age for the age of the Herminita moraines exists near Lago Pearson (or Anita) (Fig. 1), closer to Upsala Glacier. Here, a ^{14}C age from the basal section of a bog just south of Lago Pearson (Fig. 1, Table 1) indicates that the ice margin had receded to near the position of the outermost Holocene moraines prior to 9040 ± 45 ^{14}C yr BP (10,210 ± 50 cal. yr BP). In addition, the ^{14}C ages

that constrain recession from the northern arm of Lago Argentino are consistent with a date obtained for deglaciation of Brazo Sur, the southern arm of the lake (Fig. 1). Near Lago Frías at the head of Brazo Sur, an age for initial plant colonization of 10,400 ± 40 ^{14}C yr BP (12,270 ± 100 cal. yr BP) was measured on an organic sample from the basal section of a core through a peat bog situated just outboard of the oldest Holocene moraine (Fig. 1, Table 1). In sum, ^{14}C ages from the Herminita Peninsula (Fig. 2), the Lago Pearson area, and the Lago Frías area all indicate that glacier ice had to recede from over the sampled sites in both Brazo Norte and Brazo Sur by ~10,400 ^{14}C yr BP (12,000 cal. yr BP).

For the purpose of constraining the local ^{10}Be production rate, we use the ^{14}C age of 10,350 ± 45 ^{14}C yr BP (12,220 ± 110 cal. yr BP) from core AR0613, located just inboard of the Herminita moraines (Figs. 2 and S2). We adopt this age as a minimum-limiting calendar-year-converted ^{14}C age for deposition of the Herminita moraine sequence. Thus boulders situated on Herminita moraines commenced exposure to cosmic ray flux before 12,220 cal. yr BP.

2.5. ^{14}C age constraints for the Puerto Bandera moraine system

During glacier expansion through western Lago Argentino to the position of the Puerto Bandera moraines, vegetation and peat accumulations on the northern valley wall at Bahía del Quemado were overrun by ice and buried by till and lateral moraines (Strelin et al.,

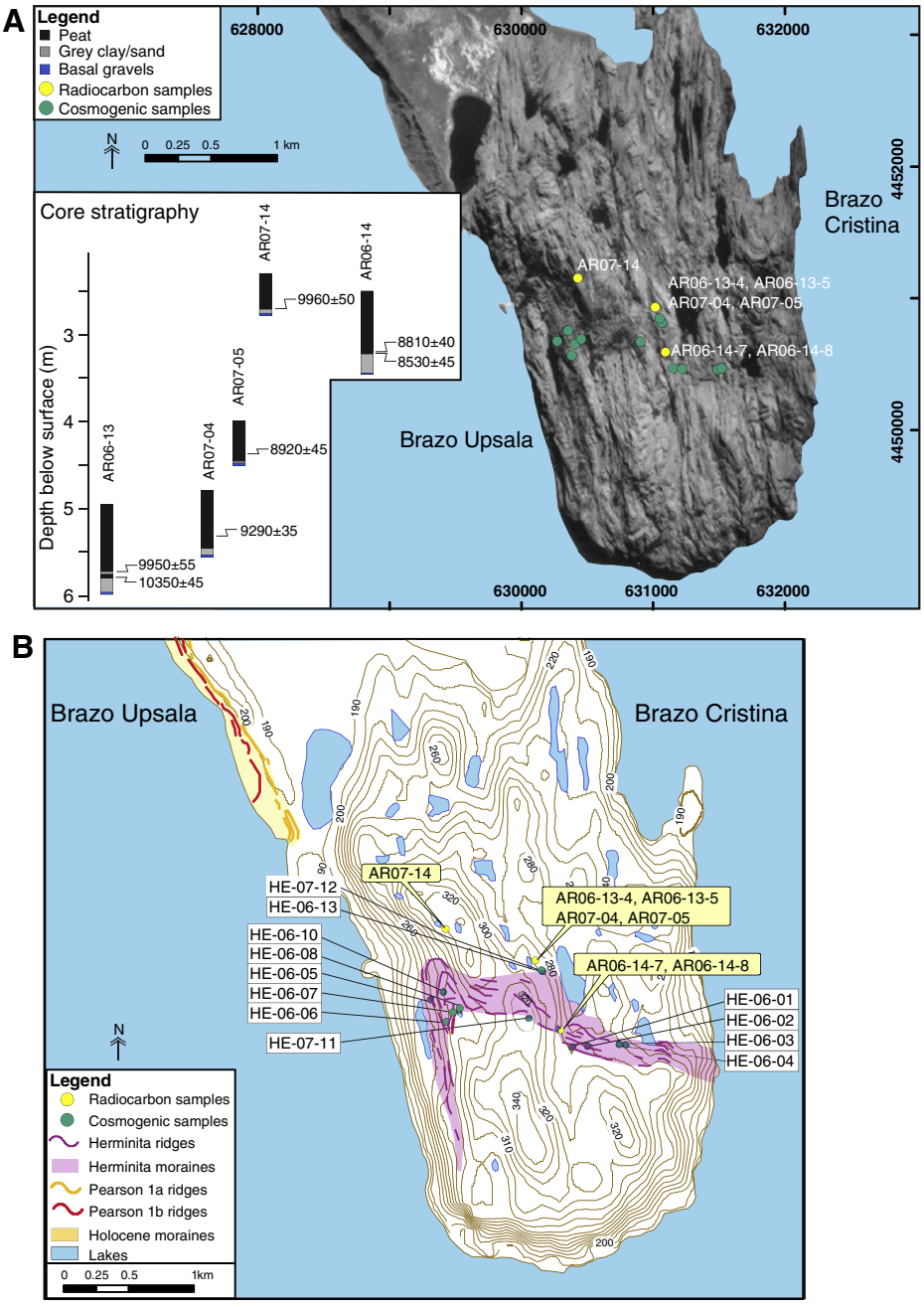

Fig. 2. The Herminita moraines and locations of ^{14}C- (yellow circle) and ^{10}B-dated samples (green circles). A) The top panel shows an aerial photograph and the details of the ^{14}C-dated cores that are relevant for understanding the ^{10}Be production rate. The legend in the upper left explains the core stratigraphy. The basal gravels are the lowermost unit encountered in each respective core. Samples for ^{14}C dating (details in Table 1) were obtained from the lower peat units of reach respective core and provide minimum-limiting ages for ice recession from the Herminita moraines. Also shown are Universal Transverse Mercator grid coordinates; B) The bottom panel displays a map of the Herminita Peninsula, with the Herminita and Holocene moraine geomorphology highlighted. The legend in the lower left defines the geomorphic features. Locations of the Puerto Bandera samples are given in the supplement (Fig. S1).

Table 1
Limiting radiocarbon ages for the Herminita moraine system (and Lago Frías area), shown in Figs. 1 and 2.

Core	Depth (cm)	Sample description	Age ± 1σ (^{14}C yr BP)	Age range (cal yr BP ± 1σ)	Mean (cal yr BP)	Age significance
Herminita Peninsula — minimum-limiting ages for formation of Herminita moraines (Fig. 2)						
AR0613	575–576	Organic sediment	10,350 ± 45	12,080–12,380	12,220 ± 110	From basal layer, peat bog development
AR0613	571–572	Organic sediment	9950 ± 55	11,250–11,600	11,410 ± 120	From basal layers, peat bog development Note that overlies above sample and is stratigraphically correct
AR0714	270	Organic sediment	9960 ± 50	11,260–11,600	11,420 ± 120	From basal layer, peat bog development
AR0704	535	Plant fragments	9290 ± 35	10,430–10,560	10,480 ± 60	From basal layer, peat bog development
AR0705	439	Plant fragments	8920 ± 45	9930–10,180	10,050 ± 90	From basal layer, peat bog development
AR0614	318–319	Bulk peat	8810 ± 40	9710–10,110	9870 ± 120	From basal layer, peat bog development
AR0614	321–322	Plant fragments	8530 ± 45	9500–9540	9510 ± 20	From basal layer, peat bog development
Lago Pearson (Anita) — minimum-limiting age for recession from Herminita Peninsula (Fig. 1)						
AR608	223	Sedge fragments	9040 ± 45	10,200–10,240	10,210 ± 50	Basal peat, minimum age for retreat from Herminita peninsula
Lago Frías area (Fig. 1)						
AR0723	258	Organic sediment	10,400 ± 40	12,150–12,390	12,270 ± 100	Basal peat, minimum-limiting age for ice retreat over the site

All ^{14}C data in this paper are from Strelin and Denton (2005), Strelin et al. (2008), and Strelin et al. (in press). Ages are calibrated to calendar years BP based on the IntCal09 curve and the OxCal 4.0.5 program (Reimer et al., 2009).

in press, Figs. 1 and S1). Prominent continuous lateral moraine belts mark the culmination of this glacier advance, and inboard moraine ridges track the recession of the Upsala ice lobe up valley toward the Herminita Peninsula shortly after the outer Puerto Bandera moraines were constructed. Strelin et al. (in press) retrieved samples of terrestrial organic material, including twigs and peat, from ancient soil surfaces buried beneath four left-lateral moraines close to the outer limit reached by Puerto Bandera ice. From these samples, Strelin et al. (in press) assayed eleven ^{14}C dates that place the mean close maximum age of the glacier advance to the outermost Puerto Bandera moraines at 11,100 ± 60 ^{14}C yr BP. This mean ^{14}C age converts to 12,990 ± 80 cal. yr BP, and constitutes a maximum-limiting date for construction of the outer Puerto Bandera moraine ridge.

Strelin et al. (in press) also describe the geologic basis for this reconstructed sequence of events during ice recession from western Lago Argentino and the Puerto Bandera moraine belt. After deposition of the moraines and subsequent ice recession from western Lago Argentino, organic accumulation commenced in bogs located on Peninsula Avellaneda, well inboard of the Puerto Bandera moraines (Fig. 1). In addition, spillways produced by overflow of an ice-dammed lake in Brazo Rico were abandoned, implying retreat of Brazo Rico ice that redirected drainage from the outer spillways to the lower Canal de los Tempanos (Mercer, 1968; Strelin et al., in press). Based on numerous ^{14}C dates, Strelin et al. (in press) determined that accumulation of organic matter at the base of bogs at Peninsula Avellaneda was underway by 12,490 ± 80 cal. yr BP, and that the Brazo Rico spillways were abandoned before 12,660 ± 70 cal. yr BP. These dates afford minimum age limits for the formation of the Puerto Bandera moraine system as a whole.

Together, maximum- and minimum-limiting age constraints place the formation of the Puerto Bandera moraines between 12,990 ± 80 and 12,660 ± 70 cal. yr BP. Therefore exposure of boulders on the Puerto Bandera moraines to cosmic ray flux commenced within this time interval.

3. Methods

3.1. Field methods

Basic mapping and description of the Herminita moraine system follows that of Malagnino and Strelin (1992), with refinements from new interpretations of aerial photographs and from field observations (Fig. 2). Detailed geomorphologic, stratigraphic, and geochronologic descriptions of the Puerto Bandera moraines can be found in Strelin et al. (in press). We carried out fieldwork to obtain samples for ^{14}C and ^{10}Be dating in the austral summers of CE2006, CE2007, CE2008, CE2009, and CE2010. Twelve samples were collected from the top sections of large stable boulders from the Herminita moraines for ^{10}Be measurements; five and four samples came from moraine segments on the west and east sides of the peninsula, respectively, and three from the moraine belt on the central part of the peninsula (Fig. 2B). The samples were from both the inner and the outer ridges of the Herminita moraines. Almost all sampled boulders are partially rooted in the moraines. Most samples are from crests of well-defined moraine ridges; two exceptions are boulders (HE-06-13, HE-07-12) located on Herminita ground moraine a few hundred meters southeast (i.e., slightly outboard) of the site of core AR0613, from which the closest minimum-limiting ^{14}C ages were obtained (Fig. 2). In addition, one sample for exposure dating was collected near the outermost (southernmost) moraine limit (HE-07-11). Close to the easternmost Puerto Bandera moraines, located about 40 km southeast of the Herminita moraines, we collected four and five samples from moraine segments on the north and south sides of Lago Argentino, respectively (Figs. S1 and S3).

For the Herminita and Puerto Bandera moraines we assume that snow cover was inconsequential on the tops of the sampled boulders for the following reasons: the moraines are close to and on the boundary of a semi arid environment, there are strong persistent westerly winds, and the tops of boulders (which have different heights above ground and different top-shapes) on the apex of moraine crests would be susceptible to winds that would remove significant snow accumulations. At present, snow cover is not persistent even in mid-winter at the low elevations (~100 to 340 m) of the sample sites (landowners, personal communication).

For the samples from the Herminita moraines, locations and elevations were measured with a Trimble ProXH GPS system relative to the WGS 1984 geographical datum, and all measurements were subsequently corrected differentially by using continuous data collected at a fixed base station (73.19147°E, 50.03076°S, 183.41 m a.s.l.). In turn, the base station was measured relative to a benchmark at Estancia Cristina established by the Argentine military (CRST 73.13235°E, 49.96341°S, 185.52 m a.s.l. referenced to Geoid). Post-processed horizontal and altitudinal uncertainties (1σ) for the samples ranged from <0.1 to 1.1 m a.s.l., and 0.1 to 0.7 m a.s.l., respectively. For the samples from Puerto Bandera moraines, locations and elevations were measured with a handheld GPS and uncertainties for elevations are assumed to be as much as ± 10 to ± 20 m. We compared elevations for each Herminita sample, taken with both the Trimble and handheld GPS,

and all agreed within 6 m, with the handheld being slightly higher in almost all cases. Accordingly, the elevation error for the Puerto Bandera moraines is assumed to be less than 20 m.

3.2. Geochemistry and analytics

Samples were processed in the Cosmogenic Nuclide Laboratory at the Lamont-Doherty Earth Observatory (LDEO). Sampling and processing followed established procedures described in Schaefer et al. (2009) and Putnam et al. (2010a). $^{10}Be/^{9}Be$ ratios were measured at the Center for Accelerator Mass Spectrometry at the Lawrence Livermore National Laboratory (CAMS-LLNL). A key aspect of this study is that we utilized recent developments in the processing and measuring of samples for ^{10}Be that allow better precision compared with previous efforts in South America and elsewhere (Schaefer et al., 2009). As a result the analytical uncertainties are typically 2–4% (Table 2).

For production-rate and age calculations, we used the methods incorporated in the CRONUS-Earth online exposure-age calculator version 2.2, with version 2.2.1 of the constants file (Balco et al., 2008; i.e., with a ^{10}Be half life of 1.36 Ma [Nishiizumi et al., 2007]). In addition, we followed changes described in Putnam et al. (2010a), Balco et al. (2009), and Goehring et al. (2010), including the high-resolution geomagnetic characterization of Lifton et al. (2008). Most ^{10}Be concentrations were measured relative to the 07KNSTD AMS ^{10}Be standard (Nishiizumi et al., 2007); four ages were measured originally relative to the KNSTD standard (see Table 2).

4. Results

4.1. ^{10}Be concentrations

The ^{10}Be concentrations (atoms/g) in twelve sampled boulders from the Herminita moraines and nine boulders from the Puerto Bandera moraines are given in Table 2 and in summary probability density plots in Fig. 3 (and Fig. S4). The surface ^{10}Be concentrations of samples from boulders on the Herminita moraines have low analytical errors (Table 2), are normally distributed, and exhibit high internal consistency, yielding a standard deviation of 4.0% (Fig. 3A). All ^{10}Be concentrations in the Herminita boulders overlap within 2σ analytical error, after standardizing to a common elevation (or sea level and high latitude; SLHL). The arithmetic mean, weighted mean, and median occur within 1σ of each other, as calculated from the ^{10}Be concentrations (Fig. 3). Hence, any of these three metrics can be used to represent the population of ^{10}Be concentrations. The result for HE-07-12 is an outlier, based on a difference from the mean of all boulder concentrations by >2 standard deviations (and Chauvenet's criterion, 95% confidence). We exclude HE-07-12 from further discussion, but stress that its inclusion would not change either the results or the conclusions given below. Leaving out HE-07-12 reduces the reduced chi-squared value (χ^2) from 2.2 to 1.6, and yields a standard deviation of 3.0% (Fig. 3B).

The surface ^{10}Be concentrations of samples from boulders on the Puerto Bandera moraines also have low analytical errors (Table 2), most of which are close to 2%. We exclude only sample EQ-08-04 from further

Table 2
Geographical and analytical data for the samples from the Herminita Peninsula and Puerto Bandera moraines.

Sample	Lat. (°S)	Long. (°W)	Elev (m a.s.l.)[a]	Thickness (cm)	Topographic shielding	$^{10}Be/^{9}Be$ (10^{-15})	Mass (g)	Be added (g)[b]	^{10}Be (atoms/g)	^{10}Be (atoms/g)[c]	$^{10}Be/^{9}Be$ ratio standard[d]
Herminita moraines											
HE-06-02	−50.0843	−73.1635	284.79	1.15	0.9998	45.5681 ± 1.0811	8.0511	0.1817	68,724 ± 1630	69,084 ± 1639	07KNSTD
HE-06-04	−50.0841	−73.1598	271.15	1.76	0.9995	42.0366 ± 1.5020	7.9359	0.1817	64,318 ± 2298	66,135 ± 2363	07KNSTD
HE-07-11	−50.0826	−73.1693	340.62	2.30	0.9999	47.1493 ± 1.0845	7.9958	0.1836	72,346 ± 1664	70,455 ± 1621	07KNSTD
HE-06-06	−50.0830	−73.1771	288.42	3.43	0.9981	41.3170 ± 1.0486	7.8544	0.1822	64,048 ± 1625	66,859 ± 1697	07KNSTD
HE-06-07	−50.0824	−73.1766	289.58	1.39	0.9997	36.0120 ± 0.9011	6.6539	0.1821	65,860 ± 1648	66,239 ± 1657	07KNSTD
HE-07-12	−50.0797	−73.1679	292.5	1.45	0.9978	40.9514 ± 1.2951	6.9161	0.1843	72,921 ± 2306	73,408 ± 2322	07KNSTD
HE-07-13	−50.0796	−73.1680	292.12	0.94	0.9997	20.5992 ± 1.3586	3.4118	0.1635	65,996 ± 4353	65,725 ± 4335	07KNSTD
HE-07-10	−50.0811	−73.1776	286.35	3.00	0.9991	40.1303 ± 1.6653	7.4870	0.1835	65,725 ± 2727	68,084 ± 2825	07KNSTD
Blank_1_2009Sep24	–	–	–	–	–	0.4799 ± 0.1921	–	0.1822	–	–	07KNSTD
HE-06-05	−50.0816	−73.1788	259.95	0.93	0.9970	109.6005 ± 2.5946	20.0769	0.1965	71,700 ± 1697	66,838 ± 1582	KNSTD
HE-06-08	−50.0821	−73.1759	284.29	1.68	0.9993	116.1638 ± 4.5108	19.2342	0.1813	73,172 ± 2841	67,195 ± 2609	KNSTD
Blank 8August06 #1	–	–	–	–	–	1.54917 ± 0.2495	–		–	–	KNSTD
Blank 8August06 #2	–	–	–	–	–	1.24866 ± 0.2577	–		–	–	KNSTD
HE-06-01	−50.0841	−73.1648	281.66	2.08	0.9995	77.4779 ± 1.7355	15.0478	0.1966	67,659 ± 1516	62,718 ± 1400	KNSTD
HE-06-03	−50.0841	−73.1605	277.46	1.67	0.9987	69.1143 ± 1.6029	12.5536	0.1947	71,651 ± 1662	66,346 ± 1533	KNSTD
Blank 28Oct06 #1	–	–	–	–	–	0.4218 ± 0.1159	–		–	–	KNSTD
Blank 28Oct06 #2	–	–	–	–	–	0.8133 ± 0.2044	–		–	–	KNSTD
Puerto Bandera moraines											
EQ-08-01	−50.17011	−72.75087	240	0.79	0.9972	67.1537 ± 1.3916	11.6080	0.1865	72,101 ± 1494	71,846 ± 1489	07KNSTD
EQ-08-06	−50.17740	−72.73030	252	1.32	0.9996	76.0799 ± 1.6961	14.0220	0.1858	67,362 ± 1502	66,713 ± 1487	07KNSTD
EQ-08-05	−50.17729	−72.72931	238	0.99	0.9990	55.7018 ± 1.1762	9.8322	0.1859	70,374 ± 1486	70,344 ± 1485	07KNSTD
PBS-08-09	−50.28208	−72.69468	221	1.86	0.9999	46.5821 ± 1.0165	8.4464	0.1872	68,998 ± 1506	70,886 ± 1547	07KNSTD
EQ-08-04	−50.17293	−72.73938	245	0.73	0.9985	43.9333 ± 1.0400	10.1220	0.1865	54,095 ± 1281	53,456 ± 1265	07KNSTD
PBS-08-04	−50.28575	−72.69151	216	0.85	1.0000	115.3671 ± 2.1024	21.1315	0.1870	68,229 ± 1243	69,285 ± 1263	07KNSTD
PBS-08-06	−50.28425	−72.68956	218	1.03	1.0000	85.3324 ± 1.8086	16.0992	0.1862	65,951 ± 1398	67,074 ± 1422	07KNSTD
PBS-08-11	−50.28002	−72.63369	215	2.06	1.0000	111.3370 ± 1.6582	21.5082	0.1862	64,409 ± 959	66,729 ± 994	07KNSTD
PBS-08-02	−50.28659	−72.69584	213	1.33	0.9999	45.6473 ± 1.2182	8.5465	0.1859	66,347 ± 1771	68,102 ± 1818	07KNSTD
Blank_1_2010Dec01	–	–	–	–	–	0.5985 ± 0.1419		0.1867			07KNSTD
Blank_2_2010Dec01	–	–	–	–	–	0.1989 ± 0.1017		0.1867			07KNSTD

Procedural blanks were processed identically with three respective batches; if two blanks were measured, average value was used for correction. AMS standards used for normalization of measurements are given in last column: KNSTD standard material: $^{10}Be/^{9}Be = 3.15 \times 10^{-12}$; 07KNSTD standard material: $^{10}Be/^{9}Be = 2.85 \times 10^{-12}$ (KNSTD:07KNSTD = 1.106 (Nishiizumi et al., 2007). Results are given with 1σ analytical AMS uncertainties.

[a] For Herminita samples, measured differentially with a Trimble Global Positioning System.

[b] LDEO Carrier 4 with a ^{9}Be concentration of 996 ppm.

[c] Same as column to the left, except concentrations are standardized, based on respective thickness and topographic shielding corrections and the average sample elevation (287 m and 229 m for the Herminita and Puerto Bandera moraines, respectively). These concentrations are shown in Fig. 3.

[d] All AMS ratio and Be concentration data presented in this Table as originally measured against the specified standard in the last column.

discussion because its ^{10}Be concentration is >2σ different from the mean, after standardizing to an average elevation of 229 m (Figs. 3C and S4B). The results for all other samples overlap at 2σ, and the mean, median, and peak concentrations overlap within 1σ of each other, as calculated from the ^{10}Be concentrations (Fig. 3). The ^{10}Be concentrations in samples from boulders in this study (Fig. 3) are indistinguishable within 1σ from those in Ackert et al. (2008), after standardizing to a common AMS standard and thickness. Sample PBS-08-11 (this study) is specifically from the same boulder as PBS-04-05 (Ackert et al., 2008); ^{10}Be concentrations are 65,520 ± 980 and 68,330 ± 4950 atoms/g relative to 07KNSTD, respectively (Fig. S4B and Table S3).

The internal coherency between individual ^{10}Be concentrations (Figs. 3 and S4) for the respective Herminita and Puerto Bandera data sets (including in Ackert et al., 2008) indicates that analytical uncertainties alone can explain the scatter of data in each distribution (Bevington and Robinson, 1992). Geomorphic processes, including erosion, inherited ^{10}Be from episodes of prior exposure, and snow cover, all of which could increase scatter, appear to be minimal.

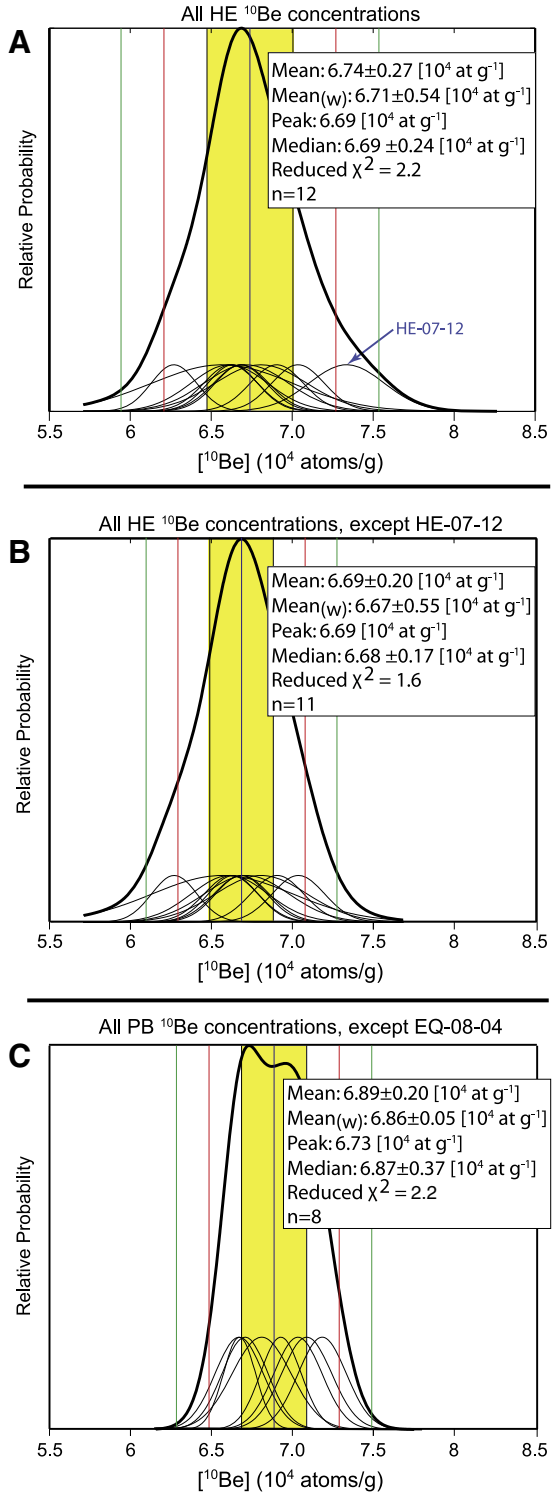

4.2. In situ production of ^{10}Be in the Lago Argentino area

A range for the local production rate can be determined from the concentrations of ^{10}Be in surface boulders from the Herminita and Puerto Bandera moraines, together with the maximum- and minimum-limiting ^{14}C ages (Table 3) for these moraines. The derived maximum-limiting ^{10}Be production rate from the Herminita moraines, which is based on a minimum-limiting ^{14}C age of 12,277 ± 110 cal. yr before CE2007, adjusted to the date on which samples for ^{10}Be analyses were collected, is <3.82 atoms/g/yr (Fig. S5) when scaled to SLHL using the Lm model (see Table 3 for other production-rate limits calculated using other scaling methods). This rate incorporates the upper error bound of the production-rate determination (i.e., +0.11 atoms/g/yr). On the other hand, the minimum-limiting ^{10}Be production rate derived from boulder-surface ^{10}Be concentrations on the Puerto Bandera moraines, and based on a calendar-year converted maximum-limiting ^{14}C age of 13,048 ± 80 cal. yr before CE2008 (also adjusted to match the date of surface-exposure sample collection), is >3.60 atoms/g/yr (also at SLHL using Lm). This rate incorporates the lower error bound of the production-rate determination (i.e., −0.08 atoms/g/yr). Likewise, the maximum-limiting ^{10}Be production rate derived from boulder-surface ^{10}Be concentrations on the Puerto Bandera moraines, and based on a calendar-year-converted minimum-limiting ^{14}C age of 12,718 ± 70 cal. yr before CE2008, is <3.87 atoms/g/yr (also at SLHL using Lm).

Altogether, in order to produce valid ^{10}Be surface-exposure ages on both the Herminita and Puerto Bandera moraine sets that satisfy all ^{14}C limits, the in-situ ^{10}Be production rate must be between 3.60 and 3.82 atoms/g/yr (Lm). The midpoint of this range is the same value as that derived from the ^{10}Be concentrations in the Herminita boulders (<3.71 ± 0.11 atoms/g/yr). Any production-rate value that is greater than or less than this range will produce untenable ^{10}Be ages for one or both of the moraine sets studied here.

5. Discussion

5.1. ^{10}Be production rate confirmation in Patagonia

^{10}Be and ^{14}C data from the Herminita and Puerto Bandera moraines of the Lago Argentino area define a range of acceptable production-rate values and afford a test of the broader applicability, at least in middle latitudes of the Southern Hemisphere, of the rate presented by Putnam

Fig. 3. Probability density plot of the Herminita and Puerto Bandera moraine boulder-surface ^{10}Be concentrations. Y-axis is relative probability. Analytical uncertainties typically of 2–4% reflect recent developments in the processing and measuring of samples for ^{10}Be, as explained in Schaefer et al. (2009). A). Concentrations in this diagram have been corrected for shielding and thickness (Table 2) and standardized to the elevation of 287 m a.s.l., the average elevation of the twelve samples (sample elevations range from 271 m to 292 m, except for HE-07-11 (341 m)). Thin curves are Gaussian representations of individual ^{10}Be, while the thicker black curve represents the summed probability of the total population. Black, red and green vertical lines mark one, two, and three standard deviations, respectively, and the center vertical blue line and yellow band denotes the arithmetic mean value ±1σ. Summary statistics are in insets. B) Same as A) except HE-07-12 is excluded (see text). C) Same as panels A and B, except concentrations in the Puerto Bandera samples (excluding obvious outlier EQ-08-04, see supplement), which have been standardized to the elevation of 229 m a.s.l., the average elevation of the nine samples (sample elevations range from 213 to 252 m).

Table 3
Comparison of production rates using scaling methods given in Balco et al. (2008), including those calculated with the ^{10}Be concentrations in boulders from the Herminita and Puerto Banderas moraines.

Herminita moraines					
Scaling scheme ID	P_{HE}/07KNSTD/Li08 (atoms/g/yr)[a]	P_{NZ}/07KNSTD/Li08 (atoms/g/yr)[b]	P_{HE}/07KNSTD/Ba08/1950 (atoms/g/yr)[c]	P_{CRONUS} (atoms/g/yr)	P_{NENA} (atoms/g/yr)
De	<3.91 ± 0.11 (3%)	3.87 ± 0.08 (2.1%)	<3.93 ± 0.12 (3%)	4.40 ± 0.53 (12%)	4.10 ± 0.20 (4.9%)
Du	<3.95 ± 0.11 (3%)	3.83 ± 0.08 (2.1%)	<3.96 ± 0.12 (3%)	4.42 ± 0.53 (12%)	4.13 ± 0.20 (4.9%)
Li	<4.21 ± 0.12 (3%)	4.15 ± 0.09 (2.2%)	<4.23 ± 0.13 (3%)	4.85 ± 0.49 (10%)	4.47 ± 0.22 (4.9%)
Lm	<3.71 ± 0.11 (3%)	3.74 ± 0.08 (2.1%)	<3.73 ± 0.11 (3%)	4.37 ± 0.39 (9%)	3.85 ± 0.19 (4.9%)

Puerto Bandera moraines				
Scaling scheme ID	$P_{PB\ min}$/07KNSTD/Li08 (atoms/g/yr)[d]	$P_{PB\ max}$/07KNSTD/Li08 (atoms/g/yr)[e]	$P_{PB\ min}$/07KNSTD/Ba08 (atoms/g/yr)[f]	$P_{PB\ max}$/07KNSTD/Ba08 (atoms/g/yr)[g]
De	>3.87 ± 0.08 (2%)	<3.98 ± 0.08 (2%)	>3.89 ± 0.08 (2%)	<3.99 ± 0.08 (2%)
Du	>3.91 ± 0.08 (2%)	<4.01 ± 0.08 (2%)	>3.92 ± 0.08 (2%)	<4.03 ± 0.08 (2%)
Li	>4.17 ± 0.09 (2%)	<4.28 ± 0.09 (2%)	>4.18 ± 0.09 (2%)	<4.29 ± 0.09 (2%)
Lm	>3.68 ± 0.08 (2%)	<3.78 ± 0.08 (2%)	>3.70 ± 0.08 (2%)	<3.79 ± 0.08 (2%)

Reference SLHL ^{10}Be production rates compared using scaling methods. All production rates shown are normalized to the 07KNSTD standard, and the values would be higher by a factor of 1.106 if given in 'KNSTD' space (Nishiizumi et al., 2007). Values in parentheses are 1σ uncertainties, which include uncertainties associated with scaling to SLHL. 'Lm' is the time dependent version of Stone/Lal scaling scheme (Lal, 1991; Stone, 2000). 'Du' is based on the scaling scheme according to Dunai (2001), 'Li' the scaling according to Pigati and Lifton (2004) and Lifton et al. (2008), and the 'De' scaling scheme is given in Desilets and Zreda (2003).

[a] For the Herminita Peninsula (P_{HE}): production rates are determined based on ^{10}Be concentrations (Table 2) and the minimum-limiting calendar-year converted ^{14}C age, adjusted to CE2007 (surface-exposure sample collection year) (Table 1) of 12,277 ± 110 cal. yr before CE2007 (10,350 ± 45 ^{14}C yr BP), and the geomagnetic framework of Lifton et al. (2008), abbreviated as Li08 (cf., Putnam et al., 2010a).

[b] The New Zealand production rates (P_{NZ}) are from Putnam et al. (2010a).

[c] The Herminita production rates (P_{HE}) presented relative to CE1950 and with the geomagnetic framework of Balco et al. (2008), abbreviated as Ba08, for comparison to the P_{CRONUS} and P_{NENA} (Balco et al., 2009) production rates, shown in columns to the right.

[d] For the Puerto Bandera moraines, minimum-limiting production rates (P_{min}) are determined based on a maximum-limiting calendar-year converted age of 13,048 ± 80 cal. yr before CE2008 (Strelin et al. in press) and Li08.

[e] For the Puerto Bandera moraines, maximum-limiting production rates (P_{max}) are determined based on a minimum-limiting age of 12,718 ± 70 cal. yr before CE2008 (Strelin et al. in press) and Li08.

[f] For the Puerto Bandera moraines, minimum-limiting production rates are determined based on a maximum-limiting age of 12,990 ± 80 cal. yr BP (Strelin et al. in press) and Ba08.

[g] For the Puerto Bandera moraines, maximum-limiting production rates are determined based on a minimum-limiting age of 12,660 ± 70 cal. yr BP (Strelin et al. in press) and Ba08.

et al. (2010a). The envelope of viable production rates in the Lago Argentina area (~3.60 to 3.82 atoms/g/yr, with a midpoint of 3.71 ± 0.11 atoms/g/yr) tightly encompasses the rate determined from Macaulay valley in the Southern Alps of New Zealand (P_{NZ}; 3.74 ± 0.08 atoms/g/yr based on Lm scaling). In other words, the P_{NZ} ^{10}Be production rate proposed by Putnam et al. (2010a) produces ages for both the Herminita and the Puerto Bandera moraine sets that are compatible with minimum- and maximum-limiting ^{14}C dates, respectively.

The range of acceptable ^{10}Be production rates to be used in Patagonia (P_{PAT}) is based on maximum- and minimum-limiting ^{14}C ages for the Herminita and Puerto Bandera moraines (Fig. 1; Table 1). On the other hand, the P_{NZ} ^{10}Be production rate calibration is based on an 'instantaneous' geological event, that is, an early Holocene debris-flow that overran trees and shrubs, which were subsequently ^{14}C dated. Moreover, Putnam et al. (2010a) confirmed that cosmogenic-nuclide production did not change significantly in New Zealand since about 18,000 cal. yr BP near the end of the last glaciation. Therefore, we conclude that the ^{10}Be production rate proposed by Putnam et al. (2010a) is appropriate for calculating accurate ^{10}Be surface-exposure ages in Patagonia.

The P_{PAT} range of production rates overlaps with rates estimated for the tropical Peruvian Andes (P_{PERU}), at 13°S and at ~4000 m elevation, under neutron-monitor-based scaling schemes calculated using data from the oldest two boulders at the pertinent site (Farber et al., 2005, calculated in Licciardi et al., 2009). The assumption in this case is that the two oldest boulders from the P_{PERU} sample set best approximate the moraine age and that the five boulders producing the younger mode of the distribution have been exhumed or eroded since moraine deposition. On the other hand, if the younger mode of the P_{PERU} boulder ^{10}Be surface-exposure ages is preferred (N = 5), and the two older dates are attributed to ^{10}Be inheritance due to prior exposure, or else attributed to deposition at an earlier time (i.e., if the moraine is indeed a composite landform produced over multiple glacier advances), or if the average of all ages obtained by Farber et al. (2005) is considered (N = 7), then Peruvian ^{10}Be and ^{14}C ages agree and we find general agreement among P_{PERU}, P_{PAT}, and P_{NZ} ^{10}Be production rates calculated using the Lm scaling scheme. There is also overlap, within stated uncertainties, among the range of acceptable P_{PAT} ^{10}Be production rates presented here and the rate derived from northeastern North America (Table 3, P_{NENA}; Balco et al., 2009), although the central tendency of the P_{NENA} rate is above the upper limit of the range of acceptable Patagonian rates. In addition, P_{PAT} is consistent with the production rate value recently determined from 69°N in northern Norway (Fenton et al., in press). However, the range of production rates derived from the Herminita and the Puerto Bandera ^{10}Be concentrations, ~3.6 to ~3.8 atoms/g/yr (Lm), is 12–15% lower than the commonly adopted 'average' production rate value (P_{CRONUS}; Balco et al., 2008), which is based on geological calibration sites available in or prior to CE2008 in the Northern Hemisphere.

As an alternative, to evaluate the use of various existing production rates in Patagonia, we also present ^{10}Be surface-exposure ages from boulders on the Herminita and Puerto Bandera moraines, calculated with different published values and four scaling schemes, in Figs. 4 and 5, respectively (Tables S1 and S2). Only the P_{NZ} rate yields ^{10}Be ages that are fully consistent with ^{14}C data. Specifically, for data from the Herminita Peninsula, use of the P_{CRONUS} rate (Fig. 4A) causes the ^{10}Be ages to be younger than the minimum-limiting ^{14}C ages from cores AR0613 and AR0714. ^{10}Be ages from Herminita Peninsula calculated with the P_{NENA} rate also are less consistent with the converted ^{14}C age of 12,277 ± 110 cal. yr before CE2007 when compared with ages calculated using P_{NZ}; seven out of twelve ^{10}Be ages overlap with the ^{14}C age, within error. For data from the Puerto Bandera moraines, use of the P_{CRONUS} rate

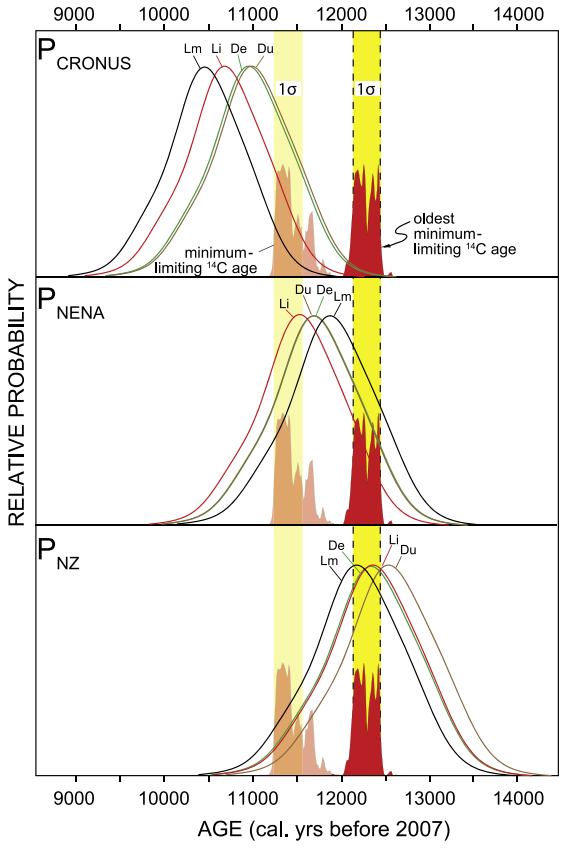

Fig. 4. Summed probability plots showing the total ^{10}Be age distribution (1σ) for the Herminita moraine sequence calculated using different production-rate calibrations and scaling schemes (see Table S1). Y-axis is relative probability. For comparison, the filled red curve and vertical yellow bands show the 1σ uncertainty ranges of the (oldest) minimum-limiting ^{14}C age of 10,350 ± 45 ^{14}C yr BP, which calibrates to a calendar age of 12,277 ± 110 cal. yr before CE2007, and minimum-limiting ^{14}C ages of 9950 ± 55 and 9960 ± 50 ^{14}C yr BP, which calibrate to 11,467 ± 120 and 11,477 ± 210 cal. yr before CE2007, respectively (all ± 1σ, Table 1).Top panel shows the ^{10}Be age distribution calculated using the 'average value' based on the calibration dataset of Balco et al. (2008, P_{CRONUS}); middle panel shows the ^{10}Be age distribution calculated with the northeast North American production rates of Balco et al. (2009, P_{NENA}); and bottom panel the ^{10}Be age distribution calculated with the Macaulay valley, New Zealand production rate (Putnam et al., 2010a). We point out that the Herminita ^{10}Be ages calculated with P_{CRONUS} are also >1σ different (Table S1) from even the calendar-year converted minimum-limiting ^{14}C ages of 11,467 ± 120 and 11,477 ± 120 cal. yr before CE2007 from cores AR0613 and AR0714 (Fig. 2A), shown by the transparent curve and band.

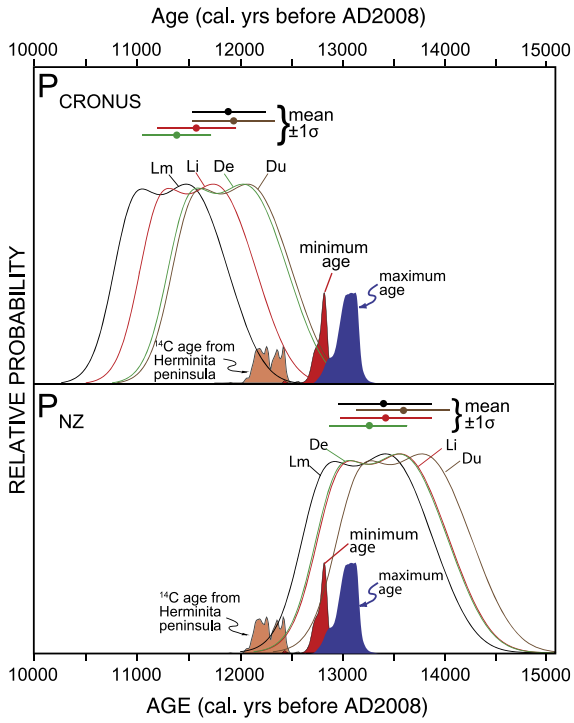

Fig. 5. Similar to Fig. 4, except probability plot showing ^{10}Be age distributions for the Puerto Bandera moraines (Table S2). Shown in blue and red are the maximum and minimum-limiting ^{14}C age calibrations for the Puerto Bandera moraine sequence, 12,990 ± 80 cal. yr BP (13,048 ± 80 cal. yr before CE2008 or 11,100 ± 60 ^{14}C yr) and 12,660 ± 70 cal. yr BP (12,718 ± 70 ^{14}C before CE2007 or 10,750 ± 75 ^{14}C yr BP), respectively (Strelin et al. in press; Strelin and Denton, 2005). Also shown is the age of 12,220 ± 110 cal. yr BP (12,777 ± 70 before CE2007 or 10,350 ± 45 ^{14}C yr BP) from the Herminita Peninsula, on a sample measured about 30 km inboard of the site, (Table 1), which affords an additional minimum-limiting age for retreat from the Puerto Bandera moraines. Top panel shows the ^{10}Be age distribution calculated using the 'average production rate' in the calibration dataset of Balco et al. (2008, P_{CRONUS}) and bottom panel calculated with production rate based on that derived in New Zealand (Putnam et al., 2010a, P_{NZ}). Note that ^{10}Be ages calculated with P_{CRONUS} are also younger, in general, than the younger ^{14}C age assayed from Herminita Peninsula, well inboard and to the northwest of the Puerto Bandera ^{10}Be sample sites (Figs. 1 and 2). Arithmetic mean age, for each respective scaling scheme, is also shown by horizontal lines above probability distributions (± 1σ).

(Fig. 5A) causes the ^{10}Be ages to be younger than the minimum-limiting date of 12,660 ± 70 cal. yr BP, and even the minimum-limiting age of 12,220 ± 110 cal. yr BP assayed from Herminita Peninsula, inboard and to the northwest of the Puerto Bandera ^{10}Be sample sites (Figs. 1 and 2).

We cannot conclude that any particular scaling scheme for latitude and elevation is 'best,' although taken at face value use of Lm may result in ^{10}Be ages that agree most closely with the ^{14}C data at the Puerto Bandera locality (e.g., Fig. 5). There are no significant age differences between scaling schemes, i.e., greater than 1σ (Balco et al., 2008; cf., Figs. 4 and 5). When P_{CRONUS} is used, age differences between scaling schemes are as high as ~4–5%, with P_{NENA} as high as 3–4%, and with P_{NZ} as high as ~3%; the variability in age between scaling schemes is reduced using P_{NZ}. The production rates from the New Zealand and South American sites overlap at 1σ, after we have scaled them to SLHL (Table 3). The apparent agreement allows confidence that each of the production rates (with uncertainties), using the respective scaling schemes, is applicable at these South American sites, which are located in the middle latitudes (~50°S). On the other hand, we acknowledge that the scaling process to SLHL, necessary to compare the site-specific production rates, introduces additional uncertainties associated with the models (e.g., Balco et al., 2008). Thus, the production rates in Table 3 from one or both sites may contain small errors related to scaling.

5.2. Late glacial events

Confirmation of a production rate in the Lago Argentino area is relevant for studies that use cosmogenic exposure ages to establish chronologies for former glacier fluctuations in Patagonia. The inferred timing of glacier advance and retreat on the Herminita Peninsula and in the Puerto Bandera area, based on both the ^{14}C and the updated ^{10}Be ages, is consistent with the timing of glacier fluctuations in the neighboring Brazo Sur area of Lago Argentino and Torres del Paine. Near Brazo Sur (Fig. 1) a minimum age of 12,270 ± 100 cal. yr BP (10,400 ± 40 ^{14}C yr BP) for plant colonization in the Lago Frías area also shows retreat from the Puerto Bandera moraines well before 12,000 cal. yr BP (Fig. 1; Table 1). Recalculated exposure ages of Ackert et al. (2008) for the Puerto Bandera moraines in western Lago Argentino (Fig. S6) are also in agreement with the ^{14}C ages presented in Strelin et al. (in press), utilizing either P_{NZ} or P_{PAT} (Table 3). The ^{10}Be ages in Ackert et al. (2008) are indistinguishable within error from data in this study for the Puerto Bandera moraines (Tables S2 and S3). Approximately 30 km to the

south of Lago Frías, in Torres del Paine, outlet glaciers from the same part of the Southern Patagonian Icefield that fed into Lago Argentino commenced retreat shortly before ~12,600 cal. yr BP from late-glacial limits (Moreno et al., 2009). Thus, three of the largest and neighboring outlet lobes of the Southern Patagonian Icefield, in the Lago Argentino/Torres del Paine region, receded after about 13,000 cal. yr BP.

Application of the P_{NZ} rate to Herminita and Puerto Bandera moraine sites in western Lago Argentino affords insights into the pan-

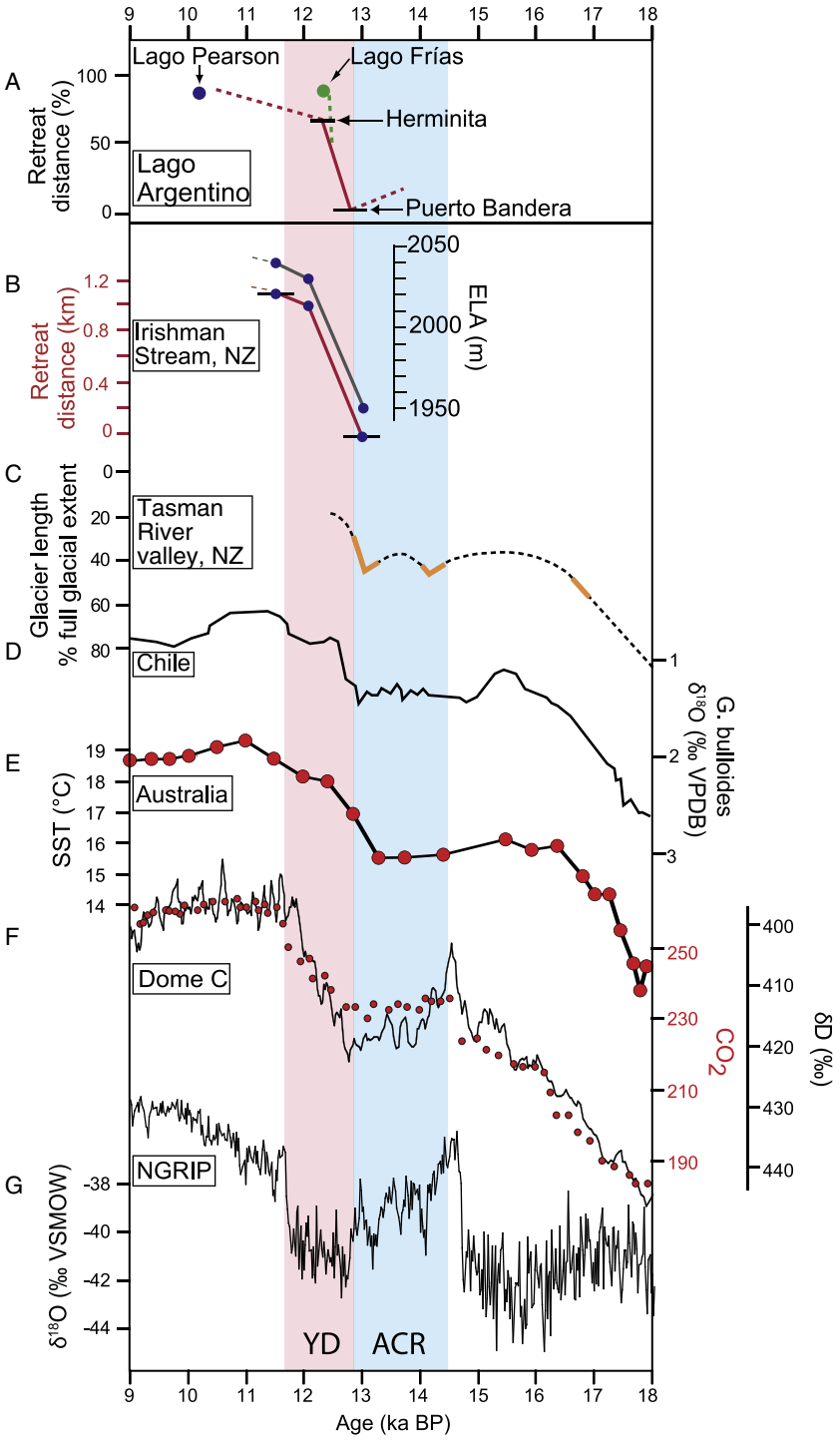

Fig. 6. Glacier changes in the Lago Argentino basin compared with other climate proxy records. From top to bottom: a) Time–distance diagram for the two major outlet glaciers in Lago Argentino, in Brazo Norte (i.e., from the Puerto Bandera moraines towards present ice margin near Lago Pearson) and near Brazo Sur (i.e., towards Frías Glacier). Age limit for the Puerto Bandera moraine event from Strelin and Denton (2005) and Strelin et al. (in press). The ages for ice recession to Lago Pearson and Lago Frías are both based on the minimum-limiting ^{14}C ages (Fig. 1, Table 1). Bold line denotes where age control exists, dotted lines are interpretations; b) The Irishman Stream valley equilibrium-line altitude and retreat distance reconstruction, South Island, New Zealand (Kaplan et al., 2010); c) Tasman River valley glacier-length reconstruction based also on ^{10}Be surface-exposure chronology (Putnam et al., 2010b). Bold lines denote where age control exists, dotted lines are interpretations; d) On the east side of the Pacific Ocean, Globigerina bulloides $\delta^{18}O$ from core ODP 1233 (Lamy et al., 2004); e) On the west side of the Pacific Ocean, South Australian alkenone-derived SSTs from core MD03-2611 (Calvo et al., 2007); f) δD (deuterium) and atmospheric CO_2 from EPICA (2004), placed on placed on timescale of Lemieux-Dudon et al. (2010); g) $\delta^{18}O$ from NGRIP (Rasmussen et al., 2006).

Pacific late-glacial history in the middle latitudes of the Southern Hemisphere (Fig. 6). With use of the P_{NZ} rate, the ^{14}C and ^{10}Be surface-exposure-age data sets fall into agreement in both the Southern Alps of New Zealand and in western Lago Argentino. In New Zealand, the age of the outer late-glacial moraine at the Birch Hill and Irishman Stream sites is ~13,000 ± 300 cal. yr before CE2007 (Fig. 6; Putnam et al., 2010b; Kaplan et al., 2010). This age is nearly identical to the calibrated ^{14}C age for the advance of Franz Josef Glacier over Caravans Knob to the Waiho Loop moraine (Denton and Hendy, 1994; Turney et al., 2007). In New Zealand and in Patagonia, ice margins retreated during the YD stadial, except for a pause around ~12,000 cal. yr BP, by which time glaciers were of smaller dimensions compared with their size at 13,000 cal. yr BP (Fig. 6A and B). Thus, a late-glacial chronology that is consistent in mountain areas in Southern Hemisphere middle latitudes on both sides of the Pacific Ocean emerges from the combined ^{14}C and exposure chronologies.

Last, the chronology of advance and retreat of mid-latitude Southern Hemisphere mountain glaciers described above is consistent with temperature reconstructions derived from Antarctic ice cores and Southern Ocean marine cores (Fig. 6). Glaciers diminished in size during the YD while temperatures increased in Antarctica (EPICA, 2004; Stenni et al., 2011) and the surrounding Southern Ocean (e.g., Anderson et al., 2009; Calvo et al., 2007; Lamy et al., 2004), and while atmospheric CO_2 concentration increased (EPICA, 2004; Lemieux-Dudon et al., 2010). The overall implication is that the late-glacial climate signal of cold and warm conditions during the ACR and YD, respectively, characterizes at least the southern quarter of the globe.

6. Conclusions

We assess the range of possible ^{10}Be production rates to use in the Lago Argentino area of Patagonia. ^{10}Be concentrations in boulders from moraines in the Lago Argentino area, which are independently dated with maximum- and minimum-limiting ^{14}C ages, can be employed to estimate a possible range for acceptable 'local' production-rate values, of ~3.60 to ~3.82 atoms/g/yr (Table 3, Lm, ±1σ) (midpoint = 3.71 ± 0.11 atoms/g/yr). This range is indistinguishable from, and tightly encompasses, the production rate recently obtained at the Macaulay site, Southern Alps, New Zealand (Putnam et al., 2010a). Based on our finding, and because the Macaulay production rate is based on an instantaneous mass wasting event, we assume the P_{NZ} rate can be used in the middle latitudes of the Southern Hemisphere. The upper acceptable limit of the local production-rate range derived at Lago Argentino is lower than the 'average' rate presented in Balco et al. (2008) by 12–15%, but also agrees within uncertainties with recent production-rate calibrations from northeastern North America (Balco et al., 2009) and northern Norway (Fenton et al., in press).

Application of the P_{NZ} rate also results in a coherent pattern of late-glacial ice-margin fluctuations on the local, regional, and hemispheric scale. ^{10}Be and ^{14}C ages in the Lago Argentino area and in the Southern Alps of New Zealand indicate glacier advance culminating late in the ACR interval, as defined in Antarctic ice cores (Blunier et al., 1997; Jouzel et al., 2001; Lemieux-Dudon et al., 2010). Exposure and ^{14}C dates both show that after the ACR advance, pronounced recession occurred during the first half of the Northern Hemisphere YD stadial. In New Zealand and in Patagonia, a pause in ice margin retreat occurred around or before 12,000 cal. yr BP (Fig. 6A and B). Finally, the updated ^{10}Be production rate for southern South America also has implications for other previously obtained datasets in Patagonia (such as for the last glaciation; see Supplementary Material).

Acknowledgments

We are grateful to the Comer family and to W.S. Broecker for their support, and also to the Instituto Antárctico Argentino (IAA) and Centro de Investigaciones en Ciencias de la Tierra (CICTERRA), and Universidad Nacional de Córdoba (UNC) for supporting the research of JS in Patagonia. We also thank the following students from the UNC and the University of Maine for field assistance: Lucas Oliva, Nadia Curetti, Juan Pablo Lovecchio, Fernando Calabozo, Mateo Martini, Juan Presta, Adrián Heredia, Samuel Kelley, and Juan Luis Garcia. For logistical support and good cheer, we thank Alejandro Tur, the skipper of Olimpo. We also thank the Estancia Cristina (Daniel Moreno), Hielo & Aventura (José Pera), and the Administración de Parques Nacionales (Guardaparque Fernando Spikermann). We thank Jeremy Frisch, Arturo Llano and Jean Hanley for laboratory assistance. Patrick Applegate and Joe Licciardi provided thoughtful and helpful reviews. This research is supported by the Gary C. Comer Science and Education Foundation, the National Oceanographic and Atmospheric Administration (specifically support to G.H.D. and M.V. for field work and ^{14}C dating), The Climate Center of LDEO and GISS, and National Science Foundation awards EAR-0902363 funded through the American Recovery and Reinvestment Act of 2009 (ARRA) and EAR-0936077. This work is LDEO contribution # 7478.

Appendix A. Supplementary data

Supplementary data to this article can be found online at doi:10.1016/j.epsl.2011.06.018.

References

Ackert, R.P., Becker, R.A., Singer, B.S., Kurz, M.D., Caffee, M.W., Mickelson, D.M., 2008. Patagonian glacier response during the Late Glacial–Holocene transition. Science 321, 392–395.

Alloway, B.V., Lowe, D.J., Barrell, D.J.A., Newnham, R.M., Almond, P.C., Augustinus, P.C., Bertler, N.A.N., Carter, L.C., Litchfield, L.C., McGlone, M.S., Shulmeister, J., Vandergoes, M.J., Williams, P.W., N.Z.-I.N.T.I.M.A.T.E. Members, 2007. Towards a climate event stratigraphy for New Zealand over the past 30,000 years (NZ-INTIMATE Project). J. Quat. Sci. 22, 9–35.

Anderson, R.F., Ali, S., Bradtmiller, L.I., Nielsen, S.H.H., Fleisher, M.Q., Anderson, B.E., Burckle, L.H., 2009. Wind-driven upwelling in the Southern Ocean and the deglacial rise in atmospheric CO_2. Science 323, 1443–1448.

Aniya, M., Sato, H., 1995. Holocene glacial chronology of Upsala Glacier at Peninsula Herminita, Southern Patagonia Icefield. 1995. Glacier research in Patagonia. Bull. Glacier Res. 13, 83–96.

Balco, G., Stone, J., Lifton, N., Dunai, T., 2008. A simple, internally consistent, and easily accessible means of calculating surface exposure ages and erosion rates from Be-10 and Al-26 measurements. Quat. Geochronol. 3, 174–195.

Balco, G., Briner, J., Finkel, R.C., Rayburn, J.A., Ridge, J.C., Schaefer, J.M., 2009. Regional beryllium-10 production rate calibration for late-glacial northeastern North America. Quat. Geochronol. 4, 93–107.

Bevington, P., Robinson, D., 1992. Data Reduction and Error Analysis for the Physical Sciences. WCB McGraw-Hill, New York. 320 pp.

Blunier, T., Schwander, J., Stauffer, B., Stocker, T., Dällenbach, A., Indermühle, A., Tschumi, J., Chappellaz, J., Raynaud, D., Barnola, J.-M., 1997. Timing of the Antarctic cold reversal and the atmospheric CO_2 increase with respect to the Younger Dryas event. Geophys. Res. Lett. 24, 2683–2686.

Calvo, E., Pelejero, C., De Deckker, P., Logan, G.A., 2007. Antarctic deglacial pattern in a 30 kyr record of sea surface temperature offshore South Australia. Geophys. Res. Lett. 34, L13707.

Casassa, G., Rivera, A., 1999. Topografic mass balance model for the Southern Patagonian Icefield. Abstract International Symposium on the Verification of Criospheric models, Bringing Data and Modeling Scientists Together, 16–20 August 1999. Zurich, p. 44.

Clapperton, C.M., 1993. Quaternary Geology and Geomorphology of South America. Elsevier, Amsterdam.

Denton, G.H., Hendy, C.H., 1994. Younger Dryas age advance of Franz Josef Glacier in the Southern Alps of New Zealand. Science 264, 1434–1437.

Desilets, D., Zreda, M., 2003. Spatial and temporal distribution of secondary cosmic-ray nucleon intensities and applications to in-situ cosmogenic dating. Earth Planetary Sci. Lett. 206, 21–24.

Dunai, T.J., 2001. Influence of secular variation of the geomagnetic field on production rates of in situ produced cosmogenic nuclides. Earth Planetary Sci. Lett. 193, 197–212.

EPICA, 2004. Eight glacial cycles from an Antarctic ice core. Nature 429, 623–628.

Farber, D.L., Hancock, G.S., Finkel, R.C., Rodbell, D.T., 2005. The age and extent of tropical alpine glaciation in the Cordillera Blanca, Peru. J. Quat. Sci. 20, 759–776.

Fenton, C.R.,Hermanns, R., Blikra, L., Kubik, P.W., Bryant, C., Niedermann, S., Meixner, A., Goethals, M.M., in press. Regional ^{10}Be production rate calibration for the past 12 ka deduced from the radiocarbon-dated Grøtlandsura and Russenes rock avalanches at 69° N, Norway, Quaternary Geochronology, doi:10.1016/j.quageo.2011.04.005.

Goehring, B.M., Kurz, M.D., Balco, G., Schaefer, J.M., Licciardi, J.M., Lifton, N.A., 2010. A reevaluation of cosmogenic $^{3}Helium$ production rates. Quat. Geochronol. 5, 410–418.

Hervé, F., Demant, A., Ramos, V.A., Pankhurst, R.J., Suárez, M., 2000. The Southern Andes. In: Cordani, U.G., Milani, E.J., Thomaz Filho, A., Campos, D.A. (Eds.), Tectonic evolution of South America. : International Geological Congress, No. 31. Río de Janeiro, pp. 605–634.

Jackofsky, D., Gosse, J.C., Cerling, T.J., Evenson, E.B., Klein, J., Lawn, B., Sharma, P., 1999. Cosmogenic nuclide chronology of LGM and post-LGM glacial history of the Southern Andes. GSA Abstracts with Programs, 31, p. A-367.

Jouzel, J., et al., 2001. A new 27 ky high resolution East Antarctic climate record. Geophys. Res. Lett. 28, 3199–3202.

Kaplan, M.R., Moreno, P.I., Rojas, M., 2008. Glacial dynamics in southernmost South America during Marine Isotope Stage 5e to the Younger Dryas chron: a brief review with a focus on cosmogenic nuclide measurements. J. Quat. Sci. 23, 649–658.

Kaplan, M.R., Schaefer, J.M., Denton, G.H., Barrell, D.J.A., Chinn, T.J.H., Putnam, A.E., Andersen, B.G., Finkel, R.C., Schwartz, R., Doughty, A., 2010. Glacier retreat in New Zealand during the Younger Dryas Stadial. Nature 467, 194–197.

Lal, D., 1991. Cosmic-ray labeling of erosion surfaces in-situ nuclide production rates and erosion models. Earth Planetary Sci. Lett. 104, 424–439.

Lamy, F., Kaiser, J., Ninnemann, U., Hebbeln, D., Arz, H.W., Stoner, J., 2004. Antarctic timing of surface water changes off Chile and Patagonian ice sheet response. Science 304, 1959–1962.

Lemieux-Dudon, B., Blayo, E., Petit, J.-R., Waelbroeck, C., Svensson, A., Ritz, C., Barnola, J.-M., Narcisi, B., Parrenin, F., 2010. Consistent dating for Antarctic and Greenland ice cores. Quat. Sci. Rev. 29, 8–20.

Licciardi, J.M., Schaefer, J.M., Taggart, J.R., Lund, D.C., 2009. Holocene glacier fluctuations in the Peruvian Andes indicate northern climate linkages. Science 325, 1677–1679.

Lifton, N., Smart, D., Shea, M., 2008. Scaling time-integrated in situ cosmogenic nuclide production rates using a continuous geomagnetic model. Earth Planetary Sci. Lett. 268, 190–201.

Malagnino, E., Strelin, J., 1992. Variations of Upsala Glacier in southern Patagonia since the late Holocene to the present. In: Naruse, R., Aniya, M. (Eds.), Glaciological Researches in Patagonia, 1990, 61–85. Japanese Society of Snow and Ice.

McCulloch, R.D., Fogwill, C.J., Sugden, D.E., 2005. Late Glacial Maxima, the Antarctic Cold Reversal and the Younger Dryas in the Strait of Magellan and Bahía Inútil; a revised chronology. Geogr. Ann. 87, 289–312.

Menéndez, C.G., Serani, V., Le Treut, H.V., 1999. The storm tracks and the energy cycle of the Southern Hemisphere: sensitivity to sea–ice boundary conditions. Ann. Geophys. 17, 1478–1492.

Mercer, J., 1968. Variations of some Patagonian glaciers since the Late glacial I. Am. J. Sci. 266, 91–109.

Mercer, J.H., 1976. Glacial history of southernmost South America. Quat. Res. 6, 125–166.

Moreno, P.M., Kaplan, M.R., François, J.P., Villa-Martinez, R., Moy, C.M., Stern, C.R., Kubik, P.W., 2009. Renewed glacial activity during the Antarctic Cold Reversal and persistence of cold conditions until 11.5 ka in SW Patagonia. Geology 37, 375–378.

Naruse, R., Skvarca, P., 2000. Dynamic features of thinning and retreating Glaciar Upsala, a lacustrine calving glacier in southern Patagonia. Arct. Antarct. Alp. Res. 32, 485–491.

Nishiizumi, K., Imamura, M., Caffee, M.W., Southon, J.R., Finkel, R.C., McAninch, J., 2007. Absolute calibration of ^{10}Be AMS standards. Nucl.Instruments Meth. Phys. Res. B 258, 403–413.

Pigati, J.S., Lifton, N.A., 2004. Geomagnetic effects on time-integrated cosmogenic nuclide production with emphasis on in situ ^{14}C and ^{10}Be. Earth Planetary Sci. Lett. 226, 193–205.

Pittock, A.B., 1980. Patterns of climatic variation in Argentina and Chile II. Temperature, 1931–60. Mon. Weather. Rev. 108, 1362–1369.

Putnam, A., Schaefer, J., Barrell, D.J.A., Vandergoes, M., Denton, G.H., Kaplan, M., Finkel, R.C., Schwartz, R., Goehring, B.M., Kelley, S., 2010a. In situ cosmogenic ^{10}Be production-rate calibration from the Southern Alps, New Zealand. Quat. Geochronol. 5, 392–409.

Putnam, A.E., Denton, G.H., Schaefer, J.M., Barrell, D.J.A., Andersen, B.G., Finkel, R.C., Schwartz, R., Doughty, A.M., Kaplan, M.R., Schlüchter, C., 2010b. The atmospheric footprint of the Antarctic Cold Reversal in southern middle latitudes. Nat. Geosci. 3, 700–704.

Rasmussen, S.O., et al., 2006. A new Greenland ice core chronology for the last glacial termination. J. Geophys. Res. 111. doi:10.1029/2005JD006079.

Reimer, P.J., et al., 2009. IntCal09 and Marine09 radiocarbon age calibration curves, 0–50,000 years cal BP. Radiocarbon 51 (4), 1111–1150.

Schaefer, J.M., Denton, G.D., Kaplan, M.R., Putnam, A., Finkel, R.C., Barrell, D.J.A., Andersen, B.G., Schwartz, R., Mackintosh, A., Chinn, T., Schlüchter, C., 2009. High-frequency Holocene glacier fluctuations in New Zealand differ from the northern signature. Science 324, 622–625.

Stenni, B., et al., 2011. Expression of the bipolar see-saw in Antarctic climate records during the last deglaciation. Nat. Geosci. 4, 46–49.

Stone, J.O., 2000. Air pressure and cosmogenic isotope production. J. Geophys. Res. 105, 23753–23759.

Strelin, J., Denton, G., 2005. Las morenas de Puerto Bandera, Lago Argentino. Proceedings of the XVI Congreso Geológico Argentino, La Plata, CD-ROM, Article 269. 6 pp.

Strelin, J., Malagnino, E., 2000. The Late-glacial history of Lago Argentino, Argentina, and age of the Puerto Bandera moraines. Quat. Res. 54, 339–347.

Strelin, J., Vandergoes, M., Kaplan, M., Denton, G., 2008. Holocene glacial chronology in the Lago Argentino Basin of the Southern Patagonian Icefield. XVII Congreso Geológico Argentino, Actas II. San Salvador de Jujuy, pp. 727–728.

Strelin, J.A., Denton, G.H., Vandergoes, M.J., Ninnemann, U.S., Putnam, A.E., in press, Radiocarbon chronology of the late-glacial Puerto Bandera moraines, Southern Patagonian Icefield, Argentina. Quaternary Science Reviews. doi:10.1016/j.quascirev.2011.05.004.

Sugden, D.E., Bentley, M.J., Fogwill, C.J., Hulton, N.R.J., McCulloch, R.D., Purves, R.S., 2005. Late-glacial glacier events in southernmost South America: a blend of 'northern' and 'southern' hemispheric climatic signals? Geografiska Annnaler 87A, 273–288.

Turney, C.S.M., Roberts, R.G., de Jonge, N., Prior, C., Wilmshurst, J.M., McGlone, M.S., Cooper, J., 2007. Redating the advance of the New Zealand Franz Josef Glacier during the Last Termination: evidence for asynchronous climate change. Quat. Sci. Rev. 26, 3037–3042.